Fermi National Accelerator Laboratory

Beams-Doc-2584
Version 1.0

The Measurements and Analysis of Electromagnetic Interference Arising from the Booster GMPS

Phil S. Yoon[1,2], Weiren Chou[1],
Howard Pfeffer[1], Steve Hays[1], Daniel A. Wolff[1]

[1] Fermilab, Batavia, IL 60510
[2] University of Rochester, Rochester, NY 14627

December 8, 2006

AD Database Keywords: Beam Instrumentation, Booster, Electronics, Power Supply, Proton Plan

Abstract

This document concerns the method of measuring common-mode voltages and current ripples arising from the Gradient Magnet Power Supplies (GMPS') of the Booster synchrotron. A series of measurements have recently been made to capture the offending interference. The aims of the measurements are to identify the type of electromagnetic interference and to diagnose main causes residing in the Booster power system.

1 Introduction

The characteristics of electromagnetic interference (EMI) are one of the most important aspects of power supplies. The EMI can be transmitted in two forms: *conductive and radiative*. The conductive EMI, such as differential-mode (DM) and common-mode (CM) noise, is usually several orders of magnitude higher than the radiative EMI, and could be more harmful to the system. Hence, the conductive EMI, particularly, the common-mode noise has been investigated. Since the common-mode voltage (V_{CM}) will be identical on both $+$ input and $-$ input of the system, it is referred to as *common-mode voltage*. As such, the common-mode voltage can be measured between two power lines ($+$ and $-$) and the ground line of the system. In order to calculate the spectra of the impulses of the common-mode noise, Fourier analysis was carried out. Note that, for convenience, all figures are placed at the end of this document.

2 Equipments

The following electronic equipments are used for the measurements:

- Agilent 54622A Oscilloscope
- Differential Amplifier
- Voltage Differentiator

3 The Measurements of Common-Mode Voltage

Figure 1 shows the waveforms of V_{+g} (potential difference between + terminal to ground) and inverted V_{-g} (potential difference between - terminal to ground). The waveform of V_{-g} is inverted for easy comparison with the counterpart. In Figure 2, for reference, the V_{CM} waveforms are plotted against the waveforms of V_{+g} and inverted V_{-g} in Figure 1.

The common-mode voltage (V_{CM}) and differential-mode voltage (V_{DM}) are calculated as follows:

$$\left.\begin{aligned} V_{CM} &= V_{+g} + V_{-g} \\ V_{DM} &= \frac{V_{+g} - V_{-g}}{2} \end{aligned}\right\} \tag{1}$$

As indicated on the upper frame of each display window in Figure 1 and Figure 2, the voltage division is set to 500 mV/div and the sweep speed to 20 ms/div with consistency. In Figures 3, 4, 5, and 6, the Fourier-analyzed common-mode voltages from GMPS [1] through GMPS [4] over 9 cycles, which correspond to the duration of 0.6 second are plotted. Based upon Figure 1 and Figure 2, it is diagnosed that the following two factors are the main causes from which the common-mode noise arises:

- phase lag between V_{+g} and V_{-g}
- amplitude (potential) difference between V_{+g} and V_{-g}

Due to the above-mentioned causes, when V_{+g} and V_{-g} are added in a point-to-point fashion, they do not cancel out each other, rather the ripples on each waveform are added up. As a consequence, the common-mode noise stands out. One of the capabilities of the given scope is to measure the peak-to-peak potential difference in each waveform (V_{+g} and inverted V_{-g}). Figures 7, 8, 9, and 10, manifest that there are substantial potential differences in V_{+g} and V_{-g} at each GMPS. Furthermore, the built-in cursor function can measure the phase lag between the two waveforms as shown in Figures 11, 12, 13, and 14. For instance, at GMPS 1, there is a phase lag of 0.6 ms between V_{+g} and V_{-g}, and the amplitude of V_{-g} is about 20 % larger than the counterpart. In case of GMPS 2, the phase lag is about 4 ms, and the fractional potential difference is 47.4 %. This implies that, as far as the phase lag and potential difference are concerned, each GMPS behaves different. The ΔV is $V_{+g} + V_{-g}$, or V_{+g} - $\mid V_{-g} \mid$. The measurements of potential differences, phase lags, and fractional potential differences at each GMPS constitute the Table 1. below: Upon measuring the signals of V_{+g}, V_{-g}, and V_{CM}, the built-in analysis function on the scope performed the fast Fourier

Table 1: Differences in voltage amplitudes and phase lags (ΔX) at each GMPS

GMPS No.	V_{+g} (V)	V_{-g} (V)	$\lvert \frac{\Delta V}{V} \rvert$	ΔX (ms)
GMPS 1	1.577	1.905	20.8 %	0.6
GMPS 2	3.232	1.699	47.4 %	4.0
GMPS 3	1.598	1.740	8.9 %	1.40
GMPS 4	1.581	1.743	10.2 %	4.60

transformation (FFT) *on the fly*. This can provide real-time proof of the presence of common-mode voltage and current ripples. The analysis results were then saved in a graphic file format. All the Figures 1 through 15 are aforementioned real-time graphic file outputs from the scope. The readings of the peak-to-peak measurements and the phase lags are shown in shaded area on Figures 7 through 14.

3.1 The Method of Fourier Analysis

The resolution of a resonant peak, or FFT bin size, is determined by FFT sampling rate (F_s) and the number of points. Since, on the oscilloscope in use, the number of points are fixed at 2048 points, the FFT sampling rates and the span of the frequency domain were controlled in accordance with the Nyquist sampling theorem. Also, in an effort to increase the resolution of the frequency peak, the Hanning window is selected over flattop, or rectangular windows. In the Figures of FFT harmonics on display, the vertical axis is in units of dBV. For reference, the FFT settings on the oscilloscope are listed as follows:

- FFT sampling rate: f_s = 3.53 kSa/s
- FFT bin size, Δf = 1.04 Hz
- Frequency-domain span = 1.67 kHz
- Scale = 20 dB/div
- Hanning window

4 The Measurements of Current Ripples

The current from the main bus line was measured by way of a transducer at GMPS 1, and then it was Fourier-analyzed. Figure 15 shows the power spectra are somewhat non-uniform distribution in the frequency domain above 15 Hz. Since the machine is driven by 15-Hz current in operation, the current is peaked at 15 Hz.

5 Concluding Remarks

The common-mode voltage induces common-mode current, which can be one of the sources of the current ripples. It is thereby suggested that more rigorous current measurements be of help by installing a more accurate current monitor on the output of the **GMPS 1**. The installation efforts can be orchestrated by the Booster group and the Electrical/Electronic Support Department.

6 Acknowledgments

One of the co-authors (Phil Yoon) would like to thank W. Chou, H. Pfeffer, S. Hays, D. Wolff, T. Morrison, and D. Buhlman for discussions and provisions made for the measurements.

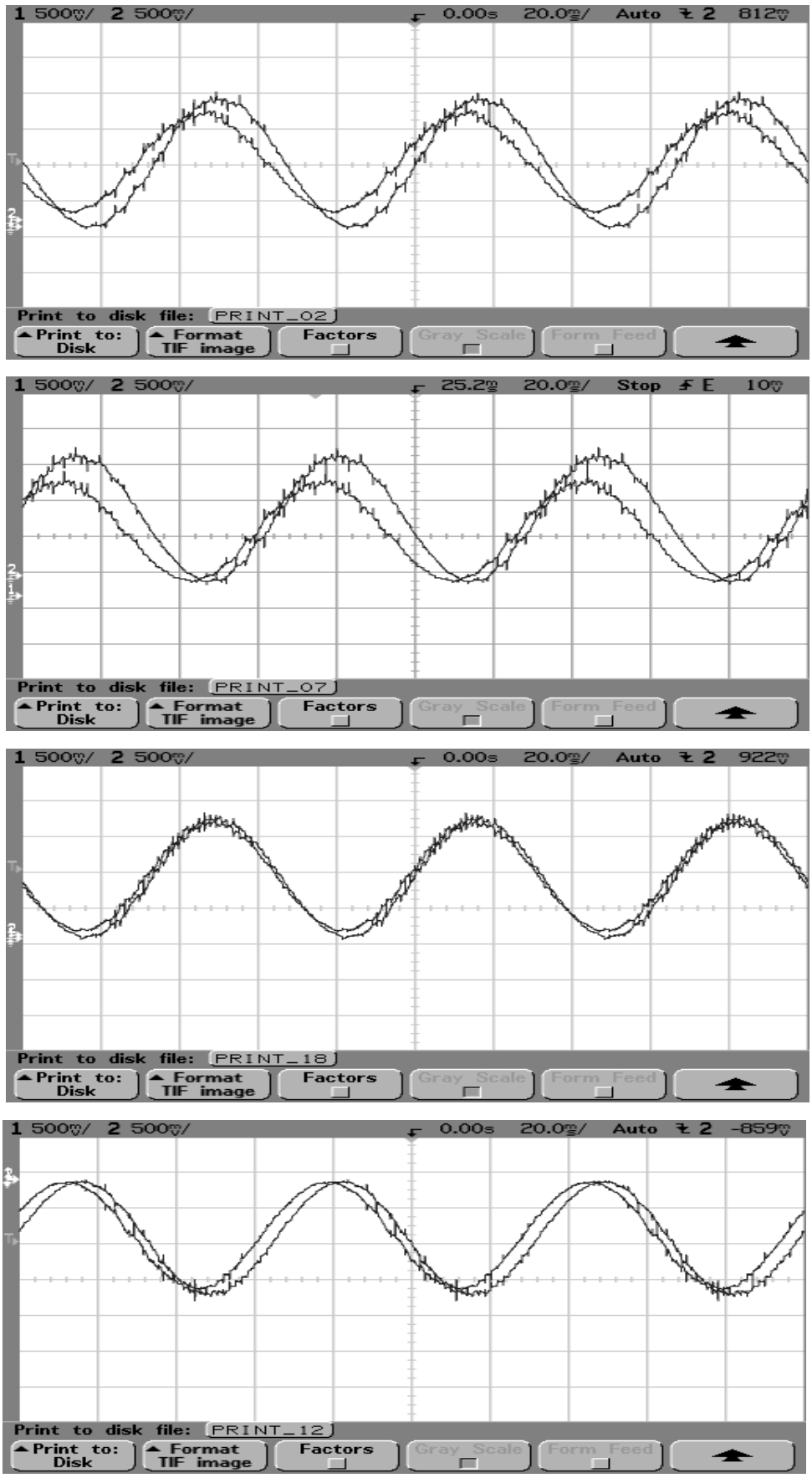

Figure 1: The waveforms of V_{+g} and inverted V_{-g}. Progressing from top to bottom, each waveform shown on the oscilloscope display corresponds to GMPS [1] through GMPS [4]. As indicated on the upper edge of each display, the voltage division is set to 500 mV/div and sweep speed to 20 ms/div.

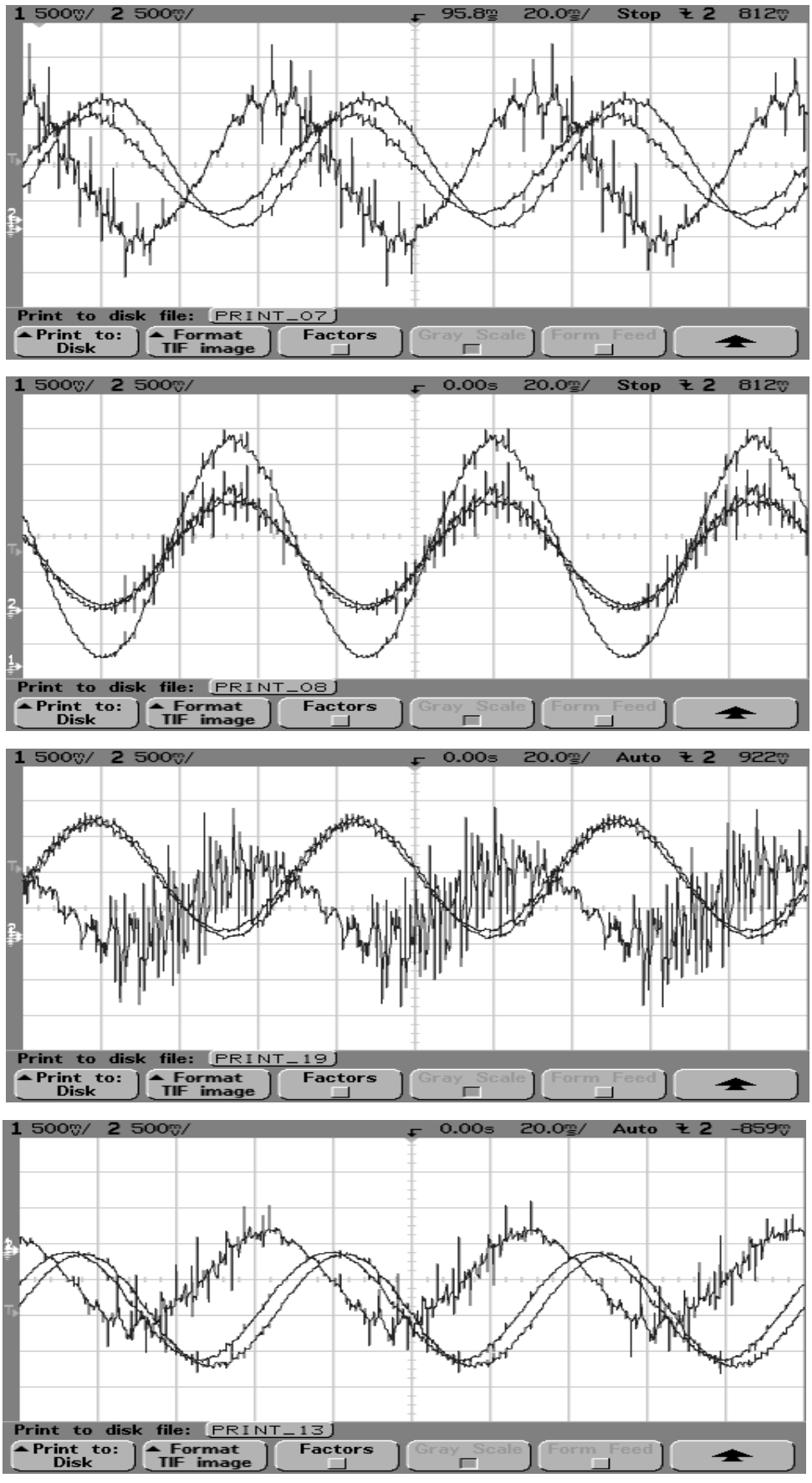

Figure 2: The waveforms of Vcm are plotted against those of V+g and inverted V-g. Starting from top to bottom, each display corresponds to the GMPS [1] through the GMPS [4]

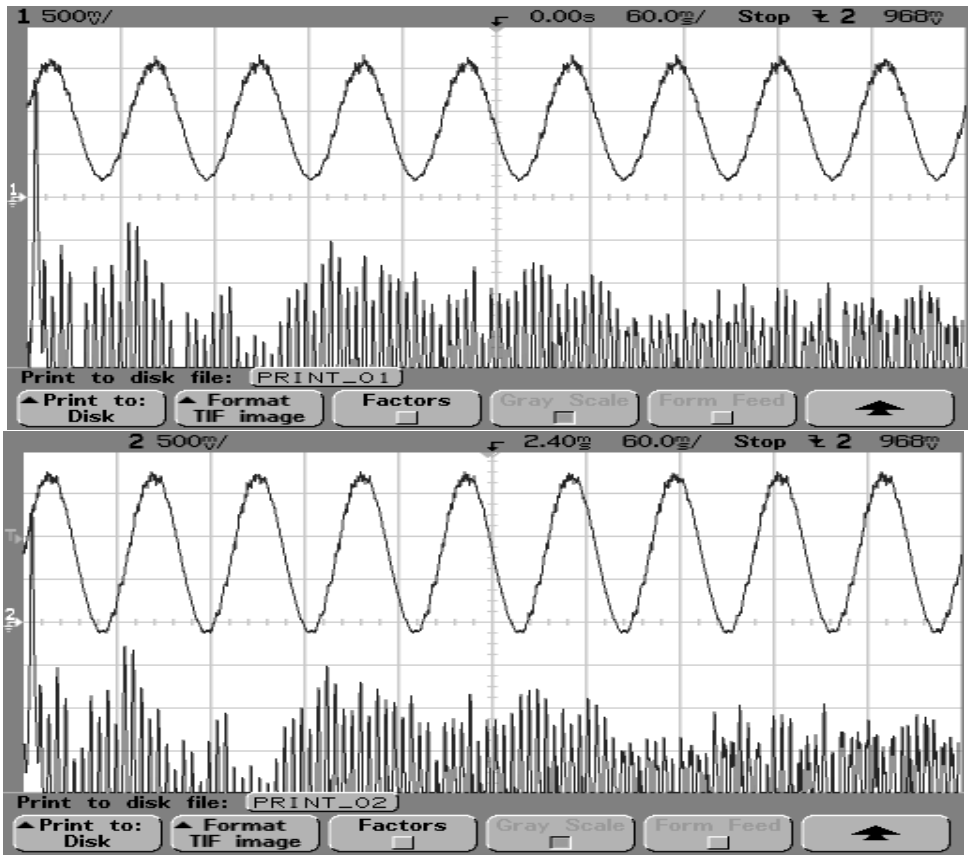

Figure 3: [**GMPS 1**] [top] The waveform of V+g and FFT power spectra; [bottom] The waveform of inverted V-g and FFT power spectra

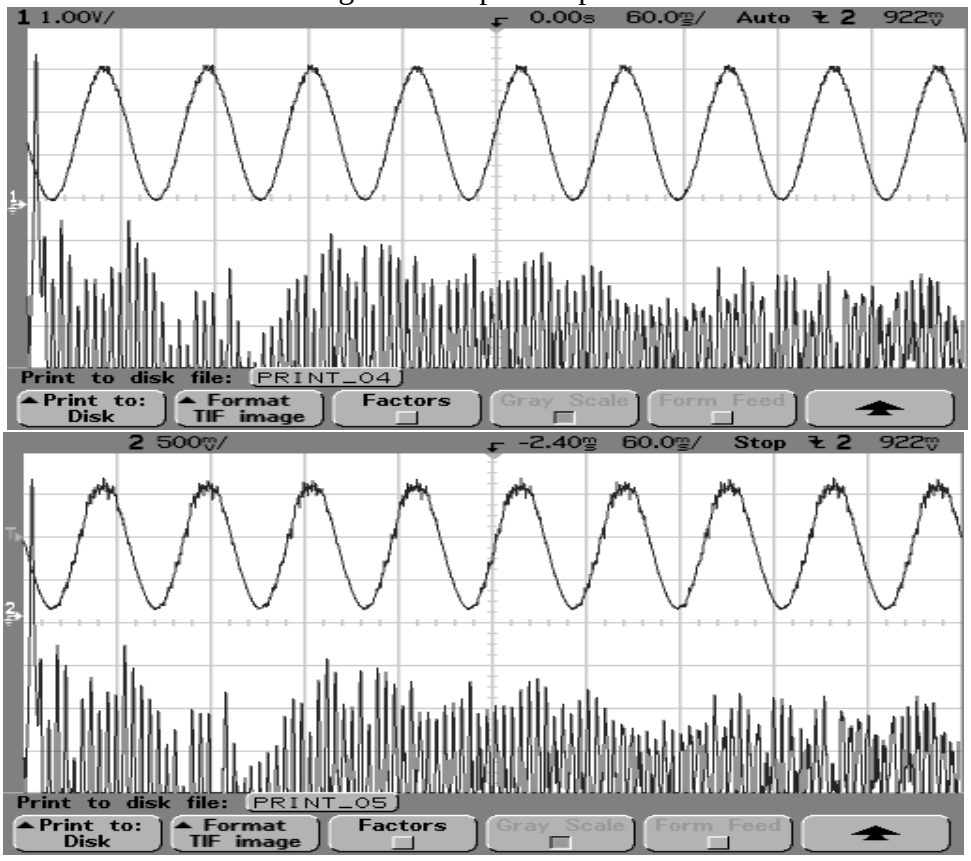

Figure 4: [**GMPS 2**] [top] The waveform of V+g and FFT power spectra; [bottom] The waveform of inverted V-g and FFT power spectra; The first resonance peak in lower frequency domain is located at 15 Hz.

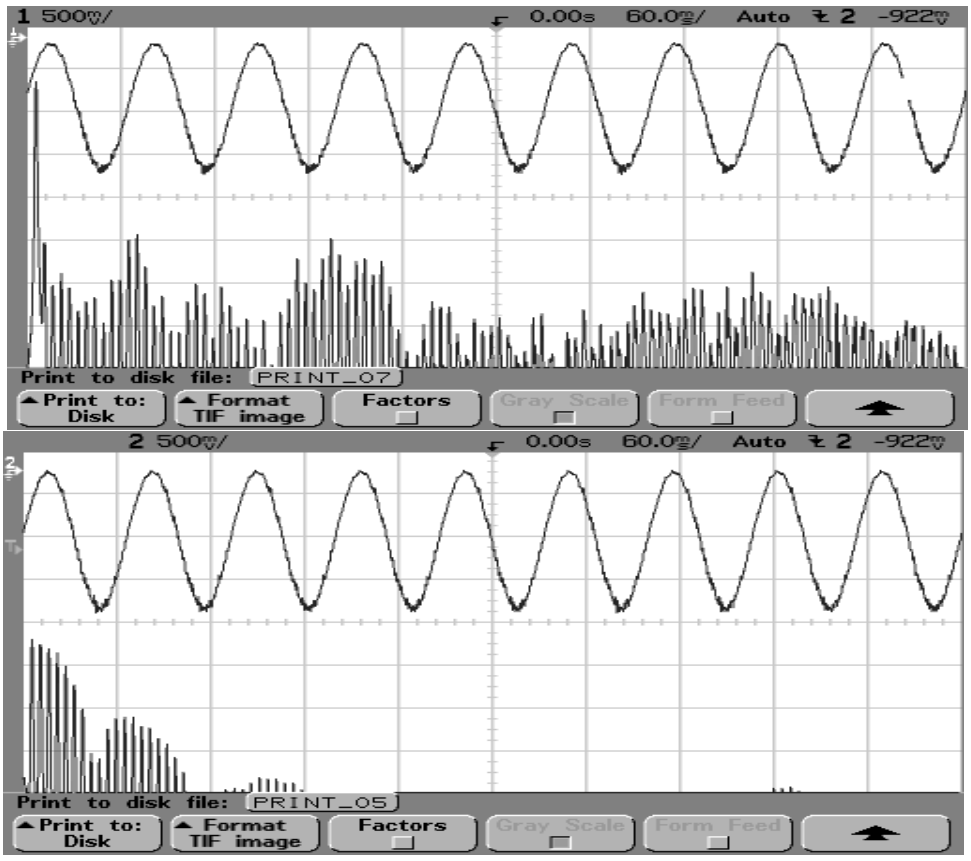

Figure 5: [**GMPS 3**] (top) The waveform and power spectra of V_{+g} and (bottom) inverted V_{-g}

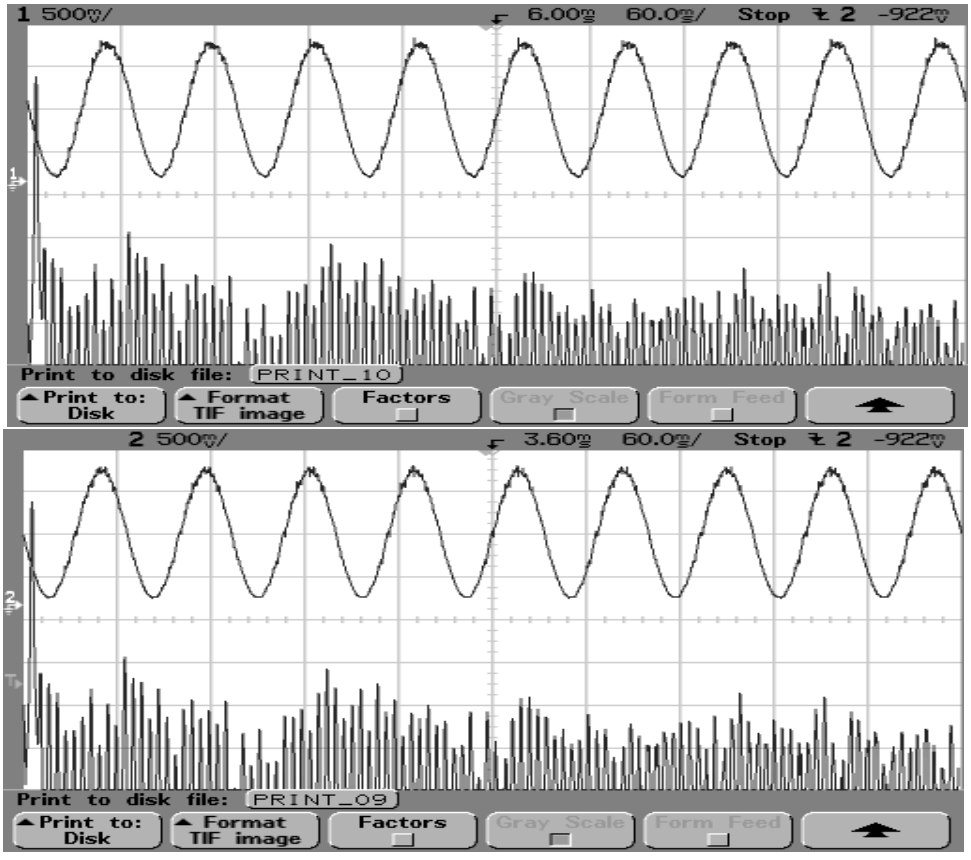

Figure 6: [**GMPS 4**] The waveform and power spectra of V_{+g} (top) and inverted V_{-g} (bottom)

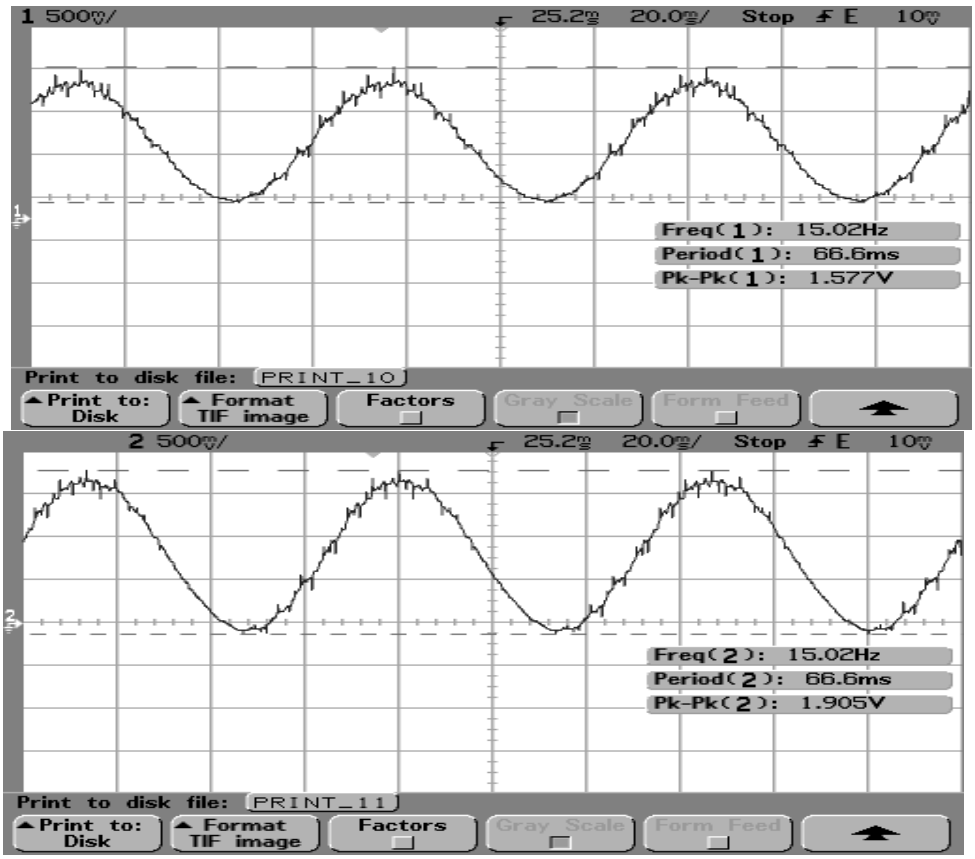

Figure 7: [**GMPS 1**] Peak-to-peak amplitude and frequency of each voltage waveform

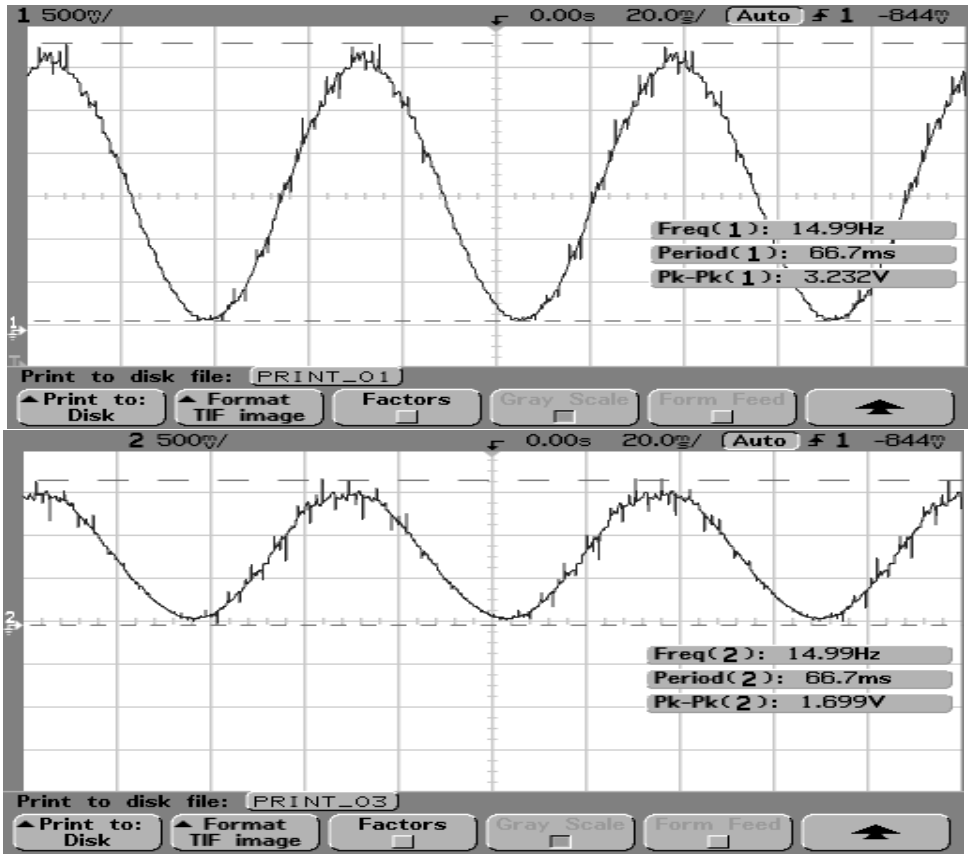

Figure 8: [**GMPS 2**] Peak-to-peak amplitude and frequency of each voltage waveform

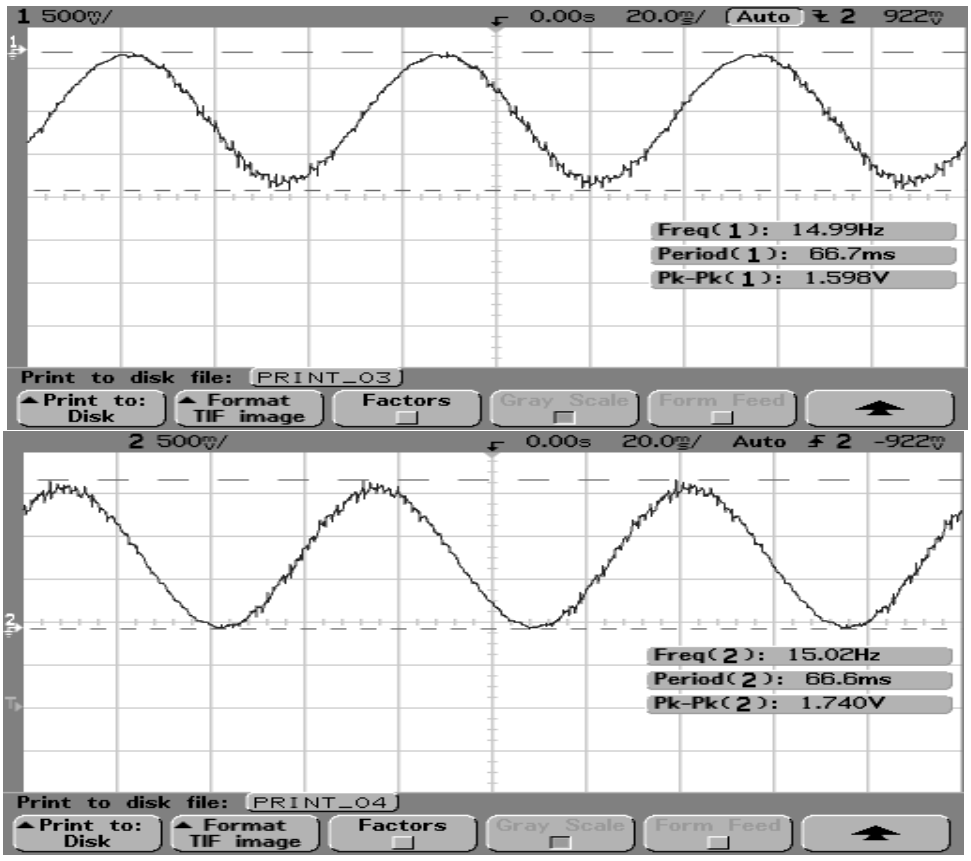

Figure 9: [**GMPS 3**] Peak-to-peak amplitude and frequency of each voltage waveform

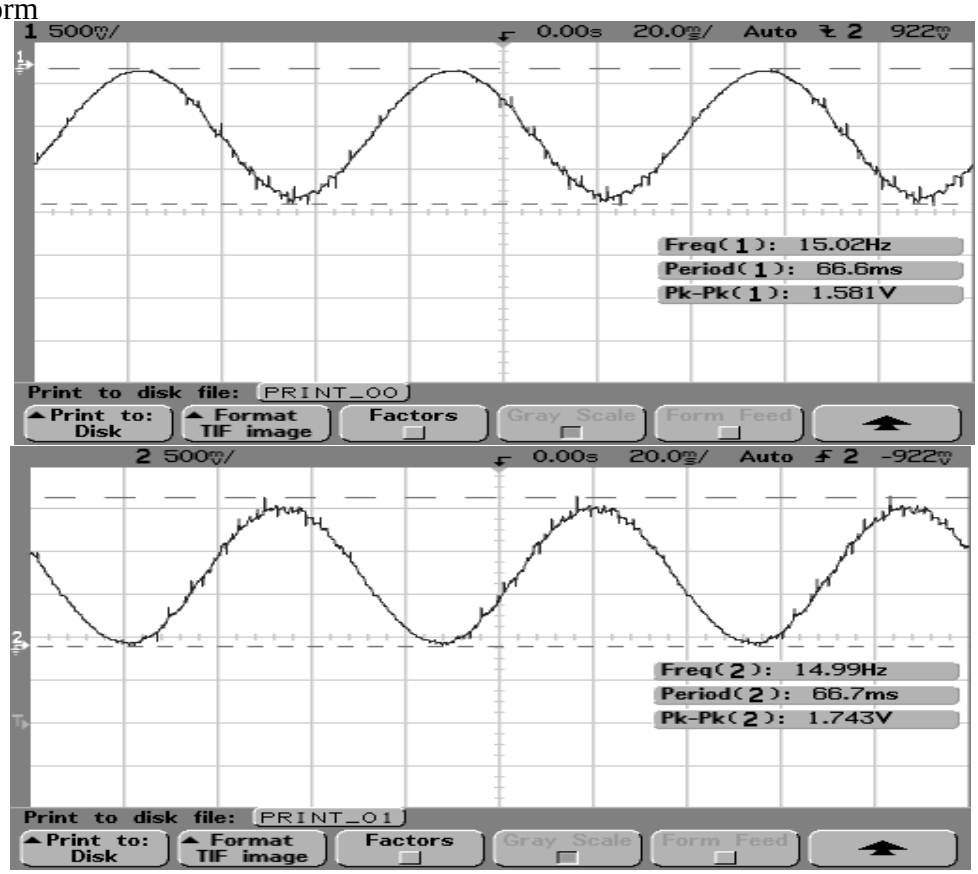

Figure 10: [**GMPS 4**] Peak-to-peak amplitude and frequency of each voltage waveform

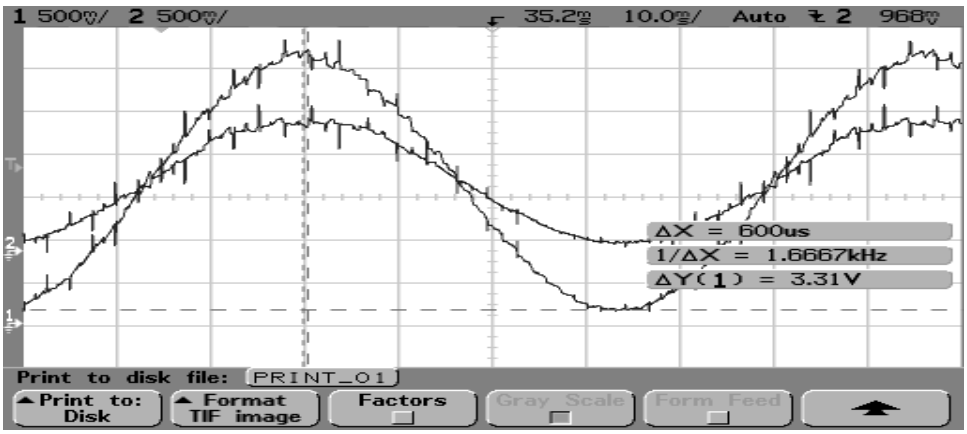

Figure 11: [**GMPS 1**] phase lag, ΔX, is 0.6 ms

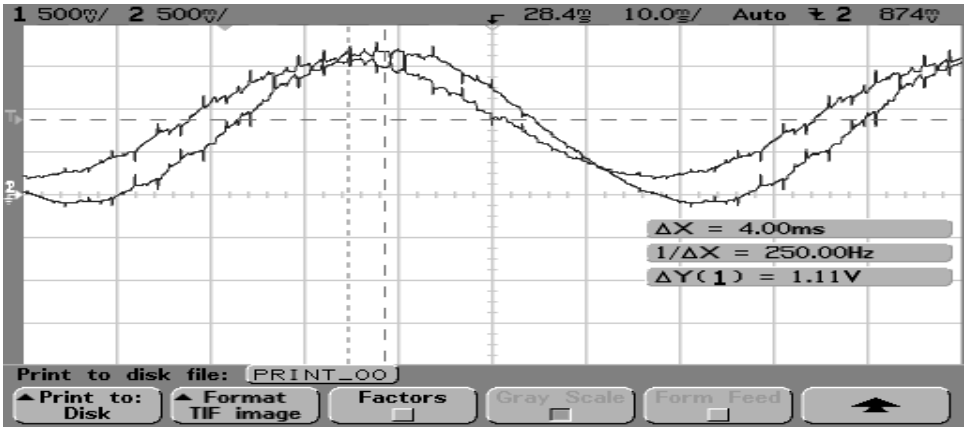

Figure 12: [**GMPS 2**] phase lag, ΔX, is 4.0 ms

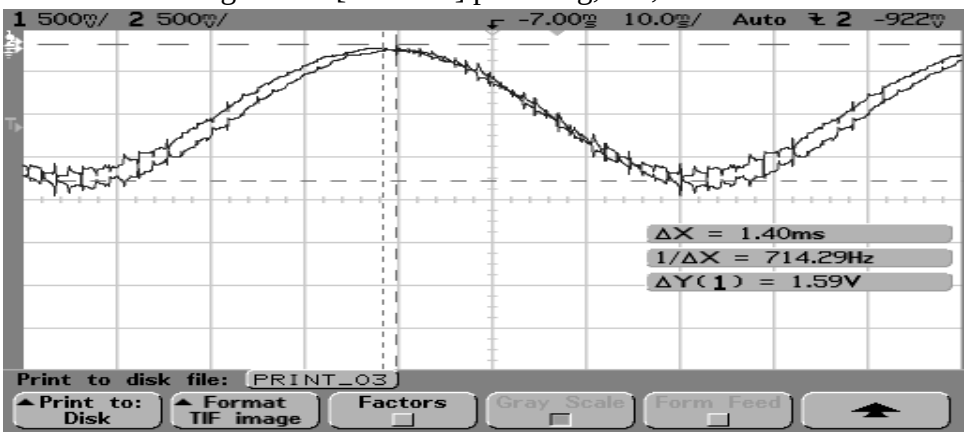

Figure 13: [**GMPS 3**] phase lag, ΔX, 1.40 ms

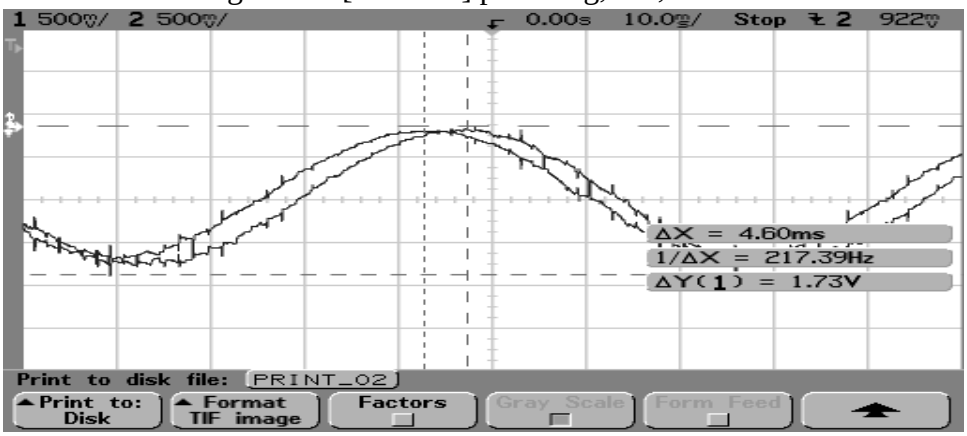

Figure 14: [**GMPS 4**] phase lag, ΔX, 4.60 ms

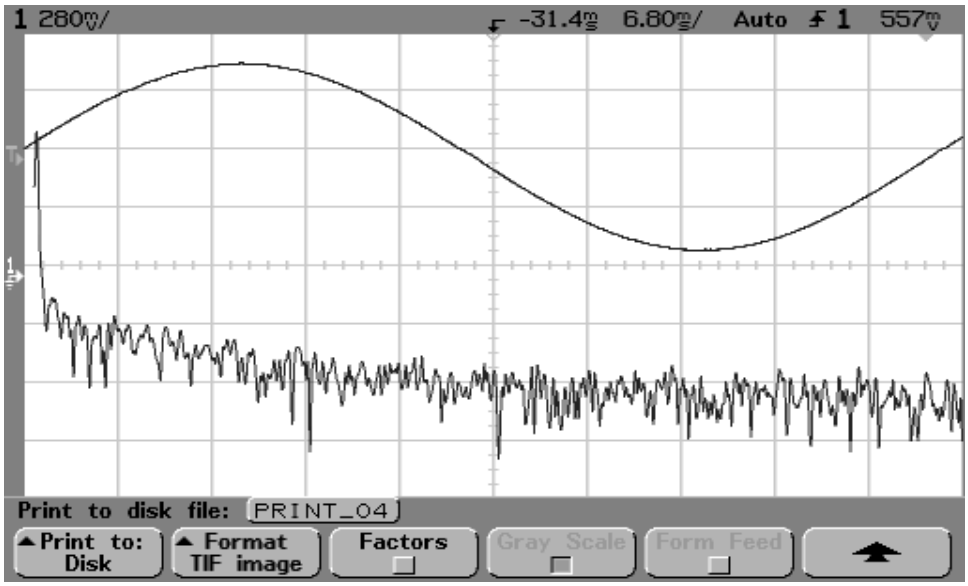

Figure 15: [**GMPS 1**] The FFT power spectra of main-bus current plotted against a current waveform